Oil Shale, 2018, Vol. 35, No. 4, pp. 327–338
doi: https://doi.org/10.3176/oil.2018.4.03
ISSN 0208-189X


# STUDY ON THE QUANTITATIVE MODEL OF THE ELASTIC MODULUS OF OIL SHALE DURING PYROLYSIS – A CASE STUDY OF FUSHUN OIL SHALE

JIAN LIU[(a,b)*], WEIGUO LIANG[(a,b)], HAOJIE LIAN[(a,b)], LI LI[(c)]

[(a)] College of Mining Engineering, Taiyuan University of Technology, Taiyuan 030024, China
[(b)] Key Lab of In-situ Property-improving Mining of Ministry of Education, Taiyuan 030024, China
[(c)] Civil and Environmental Engineering, University of Waterloo, Waterloo N2L 3G1, Canada

***Abstract.*** *The decrease of the elastic modulus of oil shale during pyrolysis was mainly caused by pyrolysis of kerogen and the deterioration of the oil shale skeleton at high temperature. Combining the thermal curve of oil shale and the change mechanism of the elastic modulus of oil shale, a quantitative model of the elastic modulus of oil shale during pyrolysis was established. The simulation results were in good agreement with the experimental data and showed that with increasing temperature, the rate and extent of decay of the elastic modulus of oil shale were gradually increased. The attenuation ratios of elastic modulus at 500 °C, 400 °C and 300 °C were approximately 68.04%, 56.42% and 48.66%, respectively.*

***Keywords:*** *oil shale pyrolysis, elastic modulus, change mechanism, quantitative model.*

## 1. Introduction

In-situ pyrolysis, which has the advantages of fewer process flows, low cost and high extraction rate, is a newly developed oil shale technology that consists in injecting heat directly into underground oil shale through injection wells. The elastic modulus of oil shale will greatly influence the permeability under the confining pressure, especially in in-situ pyrolysis conditions. The smaller the elastic modulus, the lower the permeability.

* Corresponding author: e-mail *5102135@163.com*

Thus, it is of great practical significance to study the change of elastic modulus in the pyrolysis process of oil shale.

In the past few years, researchers have investigated the mechanical properties of oil shale before or after pyrolysis, and obtained some promising results. For example, Chong [1] studied the Poisson ratio, Young's modulus and ultimate tensile strength of Green River oil shale by the split cylinder test, and found that the mechanical properties of oil shale had a linear relationship with the organic matter in oil shale. Zeuch [2] performed the constant strain rate compression tests on Anvil Points oil shale at different temperatures and confining pressures, and discovered that the strength of oil shale increased with increasing confining pressure and decreased with increasing temperature, and the ductility could be significantly improved by increasing the confining pressure. Eseme et al. [3] established that temperature had a great influence on the mechanical properties of oil shale, as both the compressive strength and the tensile strength decreased with the increase of temperature. Sun et al. [4] deemed that the release of pyrolysis products produced new complications, and the defective evolution process at the macro level was the deterioration of the mechanical properties of oil shale. Jiang et al. [5] measured the tensile strength, compressive strength, cohesive force and internal friction angle of Fuyu oil shale before and after heating. The investigators found that the mechanical properties of oil shale after pyrolysis were obviously deteriorated. Then the stress, strain and displacement of the mining area were simulated using Geostudio [5]. Jing Zhao [6] conducted uniaxial compression tests on oil shale samples from Fushun at different temperatures. The results showed that the uniaxial compressive strength, elastic modulus and the Poisson ratio decayed with the increase of temperature. Zhao also gave the corresponding fitting formulas. Guije Zhao [7] tested the mechanical properties of Jilin Yan'an oil shale at different temperatures by using a rock triaxial testing machine and ultrasonic testing instrument. The researcher found that the elastic modulus and longitudinal wave velocity of the samples generally showed a decline with increasing temperature. The elastic modulus decreased rapidly when the temperature was lower than 400 °C, when the temperature was higher than 400 °C, the descending rate of the elastic modulus slowed down, but the deceleration of the longitudinal wave velocity accelerated. Kumar and Rao [8] studied the relationship between the mechanical properties of oil shale and the temperature and organic matter content. The results showed that there was a positive correlation between the Poisson ratio and organic matter content, but the tensile strength, compressive strength and elastic modulus were negatively correlated with the content of organic matter, and the increase of temperature and organic content would lead to lower strength and Young's modulus. Dong [9] established that the tensile strength, compressive strength and elastic modulus of oil shale, as well as the Poisson ratio all decreased with increasing temperature. Glatz et al. [10] designed a high-temperature and high-pressure triaxial core holder suitable for X-ray

computed tomography (CT) scanning, and observed the formation of stress bands of Uintah Basin oil shale from room temperature to 459 °C under uniaxial compression. From the above researches it is not difficult to conclude that the mechanical parameters of oil shale deteriorate with increasing temperature, and the research on the elastic modulus mainly focuses on the comparison of these properties before and after complete pyrolysis. At the same time, the change of the elastic modulus of oil shale in the pyrolysis process has not been studied thus far. So, establishing a quantitative calculation model based on the mechanism of the change of elastic modulus is an inevitable way to study this change during oil shale pyrolysis.

## 2. Materials and methods

### 2.1. Oil shale samples and experiment procedure

The oil shale in this study was taken from the Fushun West Opencast Mine, Liaoning Province, China. The data used in the work comes from the previous studies [6, 11]. For the sake of explanation, the experimental scheme is briefly described below.

2.1.1. Thermogravimetry experiment of oil shale

First, the thermogravimetric analyser DTU-2B (Beijing Boyuan Precision Technology Development Co., Ltd) was opened, high-purity nitrogen was injected as the carrier gas, the heating rate (30 °C/min) and the final temperature (950 °C) were set, and the mass of the crucible was cleared. Then, the oil shale sample (grain size ≤ 0.2 mm) was put into the crucible, and the mass of the sample (168.63 mg) was recorded. Finally, the heating furnace was started to measure the change of the mass of the oil shale sample with the increase of temperature [11].

2.1.2. Uniaxial compression test of oil shale after pyrolysis

The large oil shale rocks were processed into Φ7.5 × 15 mm specimens, and the two ends of the specimen were polished to make the end face non-parallelity < 0.01 mm. After cutting, the samples were wrapped in aluminium foil and then placed in the furnace for pyrolysis. To avoid combustion, high-purity nitrogen was injected as the protective gas. After reaching the target temperature (20, 200, 300, 400, 500, 600 °C), the temperature was maintained until the pyrolysis product was no longer produced. Then, the specimens were cooled to room temperature and subjected to a uniaxial compression test. Three parallel samples were set at each temperature [6].

## 2.2. Research methods

### 2.2.1. Mechanism and method of the quantitative model for the elastic modulus

With the precipitation of pyrolysis products, oil shale gradually becomes porous, which causes its physical and mechanical parameters (such as the elastic modulus) to change. In this paper, it is assumed that the pore pressure during the pyrolysis of oil shale is mainly provided by kerogen. Thus, during the pyrolysis process, the decomposition of kerogen causes the pore pressure to decrease and the effective stress to increase, resulting in the change of elastic modulus and leading to the compression of oil shale. In addition, the decrease of the mechanical strength of the oil shale skeleton at high temperature also affects the elastic modulus. Based on the above analysis, the change of the effective stress and the decrease of the skeleton strength during the pyrolysis process are the main reasons for the decrease of the elastic modulus of oil shale.

Let the elastic modulus of oil shale and the compressive strength before pyrolysis be $E$ and $\sigma$, respectively. The compressive strength of oil shale and the compressive strength at any time during the pyrolysis process are $E_t$ and $\sigma_t$, respectively. The attenuation component of the compressive strength of the oil shale skeleton is $\Delta\sigma$, the pore pressure provided by kerogen pyrolysis is $\Delta u$, the compressive strength of the oil shale skeleton is $\sigma'$, and the pore pressure during the oil shale pyrolysis process is $u_t$. In the case of equal strain, equations can be established as follows:

$$\frac{\sigma}{E}=\frac{\sigma_t}{E_t}=\frac{\sigma-\Delta\sigma-\Delta u}{E_t}=\frac{\sigma'+u_t}{E_t}, \tag{1}$$

$$E_t=\frac{E\cdot\left(\sigma'+u_t\right)}{\sigma}. \tag{2}$$

### 2.2.2. Method for determining the rate equation of the pyrolysis of oil shale

In this paper, the kinetic analysis of the mass-temperature curves of oil shale pyrolysis was carried out using the Coats-Redfern (C-R) method [12–16]. The kinetic equation is as follows:

$$\ln\left[\frac{-\ln(1-\alpha)}{T^2}\right]=\ln\left[\frac{AR}{\beta D}\left(1-\frac{2RT}{D}\right)\right]-\frac{D}{RT}, \tag{3}$$

where $A$ is the frequency factor, 1/min; $D$ is the activation energy, kJ/mol; $R$ is the gas constant with a value of 8.314 J/(mol·K); $T$ is the absolute temperature, K; $\alpha$ is the conversion ratio of kerogen at temperature $T$; and $\beta$ is the heating rate, °C/min.

For most of the pyrolysis reaction temperatures and $D$ values, $D/RT >> 1$, so $(1-2RT/D) \approx 1$, and the first term on the right-hand side of Equation (3) can be considered as a constant, and the linear fitting of $\ln\left[\frac{-\ln(1-\alpha)}{T^2}\right]$ and $\frac{1}{T}$ can be performed. From the intercept $\ln\left(\frac{AR}{\beta D}\right)$ and slope $-\frac{D}{R}$ of the fitted line, the frequency factor $A$ and the activation energy $D$ can be calculated, and then the pyrolysis rate constant $k$ of oil shale at any temperature $T$ can be calculated using Equation (4):

$$k = A \cdot e^{-D/RT}. \tag{4}$$

Then, the pyrolysis reaction rate equation for oil shale at any temperature $T$ can be obtained as follows:

$$\frac{d\alpha}{dt} = k \cdot (1-\alpha). \tag{5}$$

Next, by integration of Equation (5), the functional relationship between the conversion ratio of kerogen and time at constant temperature can be found as follows:

$$\alpha = 1 - e^{-kt}. \tag{6}$$

## 3. Results and discussion

### 3.1. Results

3.1.1. Determination of pyrolysis temperature range

The TG and DTG curves of oil shale (Fig. 1) show that its pyrolysis occurred mainly in the temperature range of 300–600 °C [11]. The variation of the mechanical properties of oil shale indicates that its elastic modulus and compressive strength reduced greatly at 300–500 °C (Table 1). When the temperature rose to 600 °C, the range of change was not wide, probably due to the pyrolysis of the fixed carbon at the said temperature [6]. The variation of the elements contents of oil shale also diminished at 600 °C (Table 2) [17]. Based on the above analysis, the temperature range was determined as 300–500 °C.

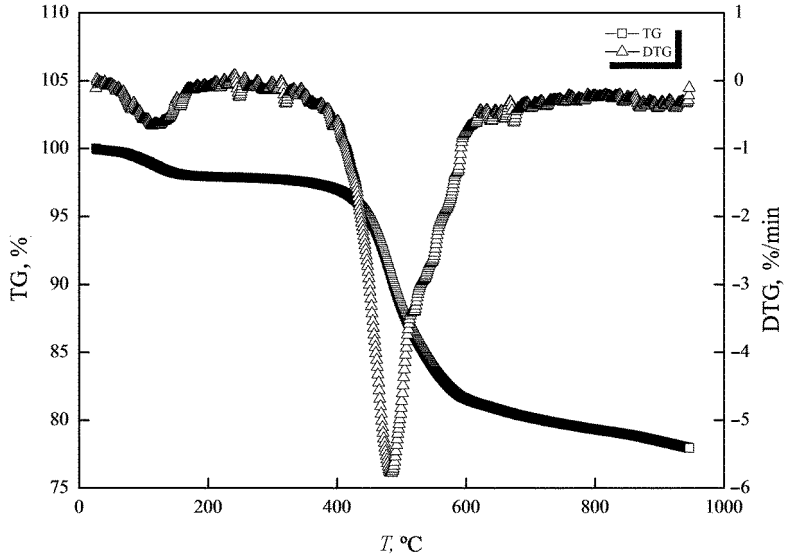


Fig. 1. TG and DTG curves of Fushun oil shale pyrolysis.

**Table 1. Mechanical properties of oil shale sample at different temperatures [6]**

| Temperature, °C | Average elastic modulus, MPa | Average compressive strength, MPa |
|---|---|---|
| 20 | 3289.33 | 76.84 |
| 200 | 2443.33 | 49.60 |
| 300 | 1748.67 | 34.28 |
| 400 | 1496.00 | 29.10 |
| 500 | 1104.67 | 21.34 |
| 600 | 1899.00 | 20.21 |

**Table 2. Elemental analysis of Fushun oil shale at different temperatures [17]**

| Temperature, °C | Elemental analysis, % | | | | |
|---|---|---|---|---|---|
| | $C_d$ | $H_d$ | $O_d$ | $N_d$ | $S_{t,d}$ |
| 20 | 16.59 | 2.57 | 6.13 | 0.71 | 0.66 |
| 300 | 8.87 | 2.17 | 6.61 | 0.61 | 0.40 |
| 400 | 7.60 | 1.36 | 6.01 | 0.60 | 0.56 |
| 500 | 5.83 | 1.08 | 3.73 | 0.45 | 0.48 |
| 600 | 4.25 | 0.48 | 0.44 | 0.31 | 0.40 |

3.1.2. Establishment of the pyrolysis reaction rate equation for oil shale

The linear fitting result of $\ln\left[\frac{-\ln(1-\alpha)}{T^2}\right]$ and $\frac{1}{T}$ in the pyrolysis stage (300–500 °C) is shown in Figure 2. Thus, the activation energy $D$ = 113012.202 J/mol≈113.01 kJ/mol, and the frequency factor $A$ =

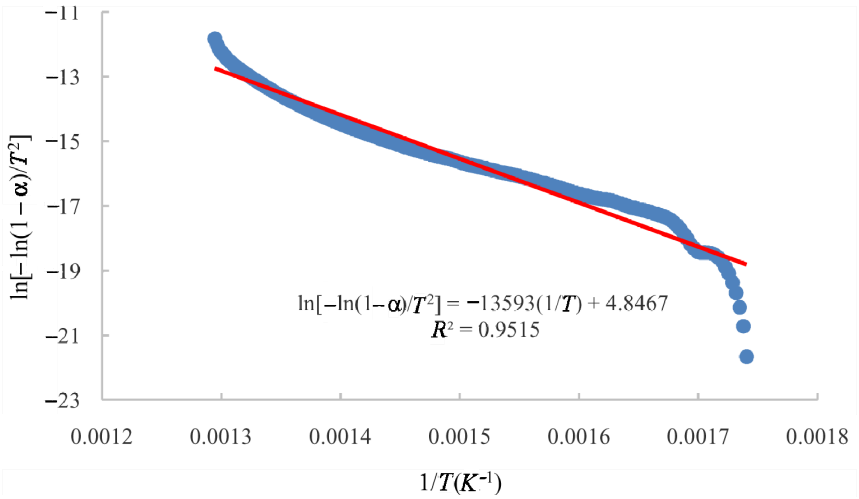


Fig. 2. Linear fitting result of $\ln[-\ln(1-\alpha)/T^2]$ and $1/T$.

51919635.76 $min^{-1}$. The reaction rate equations of oil shale pyrolysis at 300 °C, 400 °C and 500 °C can be expressed respectively as follows:

$$\alpha = 1 - e^{-kt} = 1 - e^{-2.64\times10^{-3}\cdot t}, \tag{7}$$

$$\alpha = 1 - e^{-kt} = 1 - e^{-8.92\times10^{-2}\cdot t}, \tag{8}$$

$$\alpha = 1 - e^{-kt} = 1 - e^{-1.21\cdot t}. \tag{9}$$

Previous researches [12, 13] have proved that the time required for the complete pyrolysis of oil shale decreased rapidly with the increase of temperature. The oil shale samples in this study were pyrolyzed until the pyrolysis products were no longer produced, which gave evidence of that the oil shale pyrolysis was basically completed, but the elastic modulus and compressive strength of oil shale decreased with increasing temperature. This proved that the deterioration of the mechanical properties of oil shale was caused not only by the pyrolysis of kerogen but also by the damage and weakening of the oil shale skeleton at high temperature.

### 3.1.3. Quantitative calculation of the elastic modulus of oil shale

To eliminate the influence of water on the pore pressure, the elastic modulus of oil shale at 200 °C was considered as its basic value before oil shale pyrolysis.

The compressive strengths of oil shale completely pyrolyzed at 300 °C, 400 °C and 500 °C, referred to as the oil shale skeleton compressive strengths, were determined. The results showed that the mechanical damage of the oil shale skeleton increased linearly with increasing temperature (Fig. 3). According to the fitting formula, the compressive strength of the oil

shale skeleton at 200 °C could be calculated, and then the pore pressure provided by the kerogen in the oil shale could also be found.

Based on section 2.2.1, the pore pressure in oil shale was mainly provided by kerogen. Thus, the pore pressure during pyrolysis could be calculated by combining the rate equations of oil shale pyrolysis at different temperatures given in section 2.2.2. Combining the results of the uniaxial compression test, the elastic modulus of oil shale at different pyrolysis temperatures could be found.

For example, the elastic modulus of oil shale pyrolyzed at 400 °C for 10 min was calculated, the results are presented in Table 3.

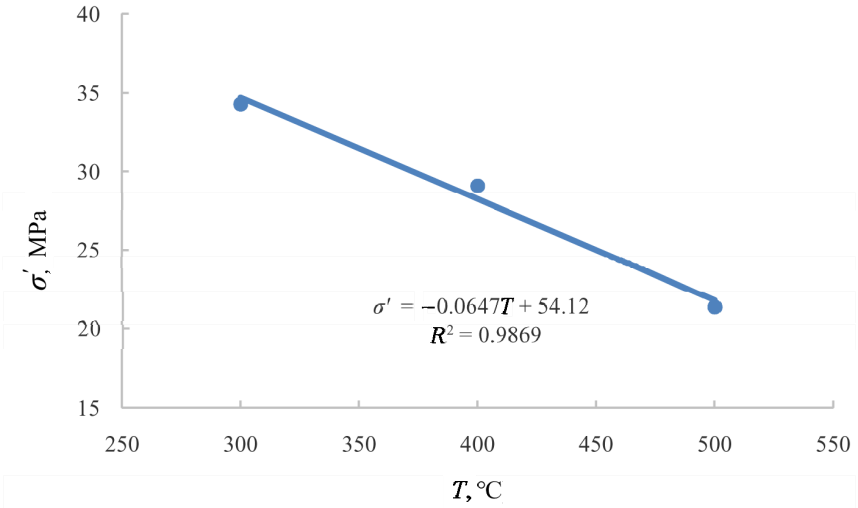


Fig. 3. Relationship between the compressive strength of the oil shale skeleton and temperature.

**Table 3. Calculation of the elastic modulus of oil shale pyrolyzed at 400 °C for 10 min**

| Parameter | Formula | Value |
|---|---|---|
| Compressive strength of the oil shale skeleton at 200 °C | $\sigma'_{200\,^\circ\mathrm{C}}$ | 41.18 MPa |
| Pore pressure provided by the kerogen in oil shale | $u = \sigma_{200\,^\circ\mathrm{C}} - \sigma'_{200\,^\circ\mathrm{C}}$ | 8.42 MPa |
| Pore pressure of oil shale pyrolyzed at 400 °C for 10 min | $u_{10\mathrm{min}} = u \cdot (1-\alpha) = u \cdot e^{-kt}$ | 3.45 MPa |
| Elastic modulus of oil shale before pyrolysis | $E = E_{200\,^\circ\mathrm{C}}$ | 2443.33 MPa |
| Compressive strength before pyrolysis | $\sigma = \sigma_{200\,^\circ\mathrm{C}}$ | 49.60 MPa |
| Compressive strength of the oil shale skeleton at 400 °C | $\sigma'_{400\,^\circ\mathrm{C}} = \sigma_{400\,^\circ\mathrm{C}}$ | 29.10 MPa |
| Elastic modulus of oil shale pyrolyzed at 400 °C for 10 min | $E_{10\mathrm{min}} = \frac{E \cdot \left(\sigma'_{400\,^\circ\mathrm{C}} + u_{10\mathrm{min}}\right)}{\sigma}$ | 1603.44 MPa |

The elastic modulus of oil shale during pyrolysis is shown in Figure 4. The decay rate of the elastic modulus decelerated as follows: 500 °C, 400 °C and 300 °C. At 300 °C, the elastic modulus was relatively moderate. At 400 °C and 500 °C, it decreased rapidly at the early stage of pyrolysis and then decayed slowly. Compared with the elastic modulus of oil shale at 20 °C, the attenuation ratio of elastic modulus at 500 °C was the highest, approximately 68.04%. At 400 °C, the decay ratio was about 56.42%, while at 300 °C, the attenuation ratio was minimum, approximately 48.66%.

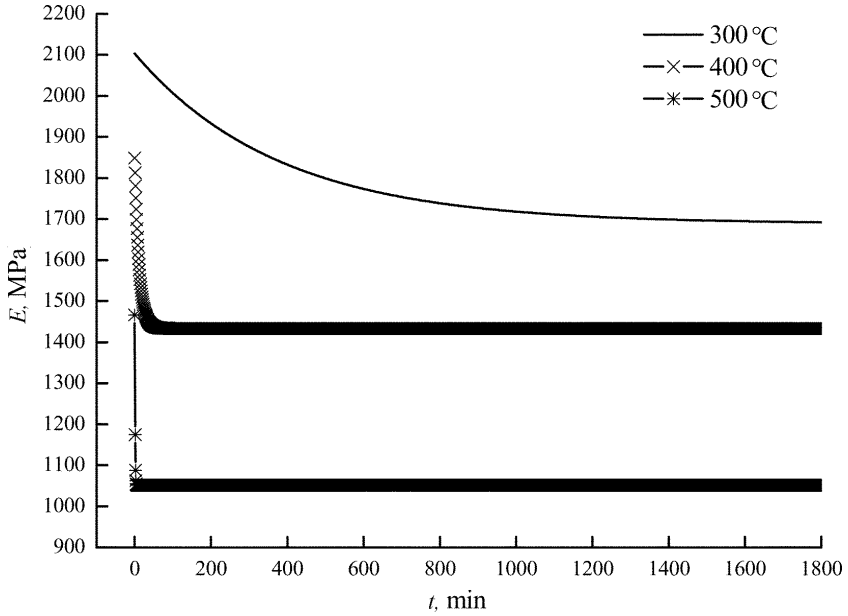


Fig.4. Elastic modulus of oil shale during pyrolysis.

### 3.2. Verification

Due to that the elastic modulus of oil shale during pyrolysis is difficult to measure, the respective values of the completely pyrolyzed rock at 300 °C, 400 °C and 500 °C were calculated and compared with the experimental values (Table 4). The results showed that the calculated elastic modulus was

**Table 4. Comparison between the calculated and experimental values of elastic modulus**

| Temperature, °C | Experimental value of elastic modulus, MPa | Calculated value of elastic modulus, MPa | Relative error, % |
|---|---|---|---|
| 300 | 1748.67 | 1688.66 | 3.43 |
| 400 | 1496.00 | 1433.49 | 4.18 |
| 500 | 1104.67 | 1051.22 | 4.84 |

very close to the experimental value, and the proposed assumption and calculation method in this paper were feasible.

### 3.3. Discussion

The verification of the results presented in section 3.2 was based on the complete pyrolysis of kerogen, but in fact, the kerogen, more or less, might remain in the pyrolyzed oil shale, which resulted in the slightly higher experimental value of the elastic modulus than its theoretical value.

In this paper, the oil shale samples were small, and so the uniform distribution of the internal temperature of the sample could be achieved in a short period. However, in actual production, due to the wide mining area, the temperature distribution of a large pyrolysis object is uneven. To simulate the variation of the elastic modulus of oil shale in a mining area, its thermal conductivity needs to be considered. Firstly, the temperature distribution and the change of the elastic modulus of oil shale should be model-found. Then, the model built in this study can be utilized to calculate the change of the elastic modulus of oil shale in the mining area.

The mechanical damage of the oil shale skeleton at high temperature was a cumulant accumulated over time. Although it would eventually converge to a constant value if the constant value was utilized in the initial stage of pyrolysis, it would cause the calculation value of the elastic modulus to be small. For a longer actual production time, this part of the error could be negligible, and the model would be applicable.

Based on the pyrolysis rate, the temperature range of 400–500 °C was the most optimum for the in-situ pyrolysis of oil shale. However, from the perspective of the elastic modulus of oil shale, high temperature would cause a great attenuation of the elastic modulus, which would more likely induce low permeability. Therefore, the excessive pursuit of pyrolysis rate was not desirable, and the optimum pyrolysis temperature should be selected by taking into account production efficiency, injection cost, environmental effects and other factors.

## 4. Conclusions

1. The decrease of the elastic modulus of oil shale during pyrolysis was mainly caused by the thermal decomposition of kerogen. The deterioration of the oil shale skeleton under high-temperature conditions was also an important reason.
2. Based on the change mechanism of the elastic modulus and the pyrolysis rate equation of oil shale, the quantitative calculation model of the elastic modulus in the pyrolysis process was established. The calculated results agreed well with the experimental data.

3. With the increase of temperature, the decay rate of the elastic modulus of oil shale was gradually accelerated, while the decay extent was gradually increased. The attenuation ratios of elastic modulus at 500 °C, 400 °C and 300 °C were approximately 68.04%, 56.42% and 48.66%, respectively.

## Acknowledgments

This work was supported by the National Natural Science Foundation of China (Grant No. 51604182).

## REFERENCES

1. Chong, K. P., Smith, J. W., Chang, B., Roine, S. Oil shale properties by split cylinder method. *J. Geotech. Eng. Div.*, 1979, **105**(5), 595–611.
2. Zeuch, D. H. The mechanical behavior of Anvil Points oil shale at elevated temperatures and confining pressures. *Can. Geotech. J.*, 1983, **20**(2), 344–352.
3. Eseme, E., Urai, J. L., Krooss, B. M., Littke, R. Review of mechanical properties of oil shales: implications for exploitation and basin modelling. *Oil Shale*, 2007, **24**(2), 159–174.
4. Sun, K., Zhao, Y., Young, D. Thermoelastoplastic damage model of heterogeneous medium and its application to thermal cracking analysis of oil shale in underground mining. *Chin. J. Rock Mech. Eng.*, 2008, **27**(1), 42–52 (in Chinese with English abstract).
5. Jiang, X., Chu, T. M., Liang, X. J., Xiao, C. L., Yan, B. Z., Wang, Y. N. Impact of mining oil shale in different methods on the environment. In: *Environment, Energy and Sustainable Development* (Sung, K. & Chen, eds.). Taylor & Francis Group, London, 2014, 359–363.
6. Zhao, J. *Experimental Study on the Microscopic Characteristics and Mechanical Property of Oil Shale under High Temperature & Three-Dimensional Stress*. PhD Thesis, Taiyuan University of Technology, 2014 (in Chinese with English abstract).
7. Zhao, G. *Study on Thermal Damage Evolution Properties and Damage Model of Oil Shale*. PhD Thesis, Jilin University, 2015 (in Chinese with English abstract).
8. Kumar, A., Rao, K. S. Engineering behavior of oil shale at elevated temperature and confining pressure. In: *5th Young Indian Geotechnical Engineers Conference*. Vadodara, India, 2015, 102–109.
9. Dong, F. Review of oil shale thermal physical property research. *Petrochem. Ind. App*., 2016, **35**(2), 1–4 (in Chinese with English abstract).
10. Glatz, G., Lapene, A., Castanier, L. M., Kovscek, A. R. An experimental platform for triaxial high-pressure/high-temperature testing of rocks using computed tomography. *Rev. Sci. Instrum.*, 2018, **89**(4), 045101, doi: 10.1063/1.5030204.
11. Kang, Z. *The Pyrolysis Characteristics and In-situ Hot Drive Simulation Research That Exploit Oil-Gas of Oil Shale*. PhD Thesis, Taiyuan University of Technology, 2008 (in Chinese with English abstract).

12. Guo, S., Geng, L. Study on pyrolysis kinetics of oil shales by thermogravimetry. *J. Fuel. Chem. & Tech.*, 1986, **14**(3), 21–27 (in Chinese with English abstract).
13. Geng, L., Guo, S. The kinetics of the thermal decomposition of Huadian oil shale by thermogravimetry. *J. Dalian Univ. Tech.*, 1984, **23**(4), 39–44 (in Chinese with English abstract).
14. Yang, J. Thermogravimetric investigation of Maoming oil shale pyrolysis kinetics. *J. China Univ. Petrol (Edition of Natural Science)*, 1982, 3, 85–93 (in Chinese with English abstract).
15. Coats, A. W., Redfern, J. P. Kinetic parameters from thermogravimetric data. *Nature*, 1964, **201**, 68–69.
16. Weitkamp, A. W., Gutberlet, L. C. Application of a micro retort to problems in shale pyrolysis. *Ind. Eng. Chem. Proc. Des. Dev.*, 1970, **9**(3), 386–395.
17. Geng, Y. *Experimental Study on the Physical and Mechanical Properties of Oil Shale during In-situ Fracturing and Pyrolysis*. PhD Thesis, Taiyuan University of Technology, 2018 (in Chinese with English abstract).

*Presented by S. Li*
Received April 17, 2018